Molecular and cellular characterization of cardiac overload-induced hypertrophy and failure

Umar, S.

Citation

Umar, S. (2009, June 18). *Molecular and cellular characterization of cardiac overload-induced hypertrophy and failure*. Retrieved from https://hdl.handle.net/1887/13860

Chapter 7

Intravenous cell therapy with mesenchymal stem cells from donor rats with pulmonary hypertension reduces right ventricular pressure overload and reverses right ventricular hypertrophy in recipient rats with pulmonary artery hypertension

S. Umar
P. Steendijk
Y. P. de Visser
G. T. M. Wagenaar
C. I. Schutte
W. H. Bax
E. Mantikou
D. A. Pijnappels
D. E. Atsma
M. J. Schalij
E. E. Van der Wall
A. van der Laarse

Abstract

Background: Pulmonary artery hypertension (PAH) is characterized by progressive increase in pulmonary artery pressure leading to right ventricular (RV) hypertrophy, RV failure and sudden cardiac death. Standard treatment is still inadequate for PAH. Stem cell therapy may constitute a new treatment modality for PAH patients.

Purpose of the study: To test whether administration of bone marrow-derived mesenchymal stem cells (MSCs) obtained from donor rats with monocrotaline (MCT)-induced PAH to rats with MCT-induced PAH resulted in (***i***) decreased pulmonary artery pressure, (***ii***) reversal of RV hypertrophy (RVH), and (***iii***) improvement of RV function.

Methods: At day 1, healthy female Wistar rats received PBS (group 1, n=10) or 60 mg/kg subcutaneous MCT (groups 2-4, each n=10) to induce PAH. At day 14, group 1 (Control) and group 2 (untreated PAH) received intravenous injection of PBS, group 3 (MSC-treated PAH) received 10^6 MSCs (group 3), and group 4 (SF-treated PAH) received 10^6 skin fibroblasts. MSCs were obtained from donor rats which received MCT (60 mg/kg) 28 days prior to bone-marrow harvesting. SFs were obtained from healthy rats. At day 28 the rats were instrumented to assess, RV function by combined pressure-conductance catheter. Subsequently, rats were sacrificed. RVH was quantified by weighing the RV free wall relative to the LV including the interventricular septum (IVS). Immunohistochemistry was performed to assess changes in the extracellular matrix of the RV.

Results: Comparing group 2 vs 1 indicated that MCT induced PAH (42±17 vs. 27±5 mmHg, p<0.05), RVH (RV/(IVS+LV) weight ratio of 0.47±0.12 vs. 0.25±0.04, p<0.001) and depressed LV ejection fraction (43±6% vs. 56±11%, p<0.005). MSC treatment (group 3) limited PAH (31±4 mmHg; p=0.08 vs. group 2), RVH (0.32±0.07; p<0.005 vs. group 2), and normalized RV ejection fraction (52±5%; p<0.005 vs. group 2). In group 4, treatment effects on RV pressure, RVH and RV function were less pronounced than in group 3.

Conclusion: Treatment with intravenous administration of MSCs obtained from donor rats with PAH reduced pressure overload, hypertrophy and RV dysfunction in rats with MCT-induced PAH. These results suggest that patients with PAH may be treated successfully using autologous MSCs.

Introduction

Pulmonary arterial hypertension (PAH), which refers to a progressive increase in pulmonary artery pressure, is a chronic debilitating disease leading to right ventricular (RV) hypertrophy, RV failure and eventually to death [1]. PAH is characterized by a progressively severe symptomatology of dyspnea, fatigue, chest pain, syncope, and right heart failure.

In a study on novel therapeutic options for patients with PAH, we have employed the monocrotaline (MCT)-induced rat model of PAH, a model which is widely used in experimental studies [2,3]. The consequences of two doses of MCT (30 and 80 mg/kg) on RV function at 28 days after MCT administration were dose-dependent (*i*) RV hypertrophy, (*ii*) RV dilatation, and (*iii*) impairment of systolic function, without marked effects on RV diastolic function [4]. Earlier, we demonstrated that tenascin-C, an extracellular matrix protein that is absent in normal myocardium, is abundantly expressed in RV myocardium of rat hearts with MCT-induced PAH [5]. In the heart, extracellular matrix proteins are predominantly secreted by fibroblasts, whereas the matrix degrading enzymes are produced by many cell types, such as fibroblasts, cardiomyocytes and macrophages. In patients with severe heart failure myocardial expression of collagenases, like matrix metalloproteinase-1 (MMP1) mRNA, was increased [6], and decreased after implantation of a left ventricular assist device (LVAD) [7]. In analogy, in the failing heart supported by LVAD also other myocardial collagenases, such as cathepsin K, demonstrated decreased concentrations [8].

The model of MCT-induced PAH is extremely useful to test new drugs to treat PAH and to study their mechanisms of action [9]. Many treatment options for PAH have been tested so far, but an effective therapy is lacking. Cell therapy constitutes a novel therapeutic option for PAH patients. Several groups have tested various cell types to treat experimental PAH, including mesenchymal stem cells (MSCs). MSCs are unique in possessing (*i*) a potential to differentiate into other cell types, and (*ii*) an ability to secrete paracrine factors leading to improvements in tissue injury [10].

Intravenous (i.v.) infusion of autologous endothelial progenitor cells (EPCs) to patients with idiopathic PAH was shown to be safe and to have beneficial effects on exercise capacity and pulmonary hemodynamics [11]. I.v. infusion of bone marrow-derived EPCs from Fisher-344 rats, cultured in endothelial growth medium for 7-10 days, to syngeneic rats 3 days after MCT administration nearly completely prevented the increase in RV systolic pressure. EPCs were recovered in the distal pulmonary arterioles and incorporated into the endothelial lining of the MCT-injured lung. Delayed i.v. injection of EPCs 3 weeks after MCT administration prevented the further progression of PAH in the following 2 weeks [12]. However, i.v. injection of unfractionated bone marrow-derived cells from donor rats to rats with MCT-induced PAH plus unilateral pneumonectomy had no beneficial effect on PAH, pulmonary arterial remodeling, and survival [13]. I.v. injection of rat bone marrow-derived mesenchymal stem cells (MSCs) to rats that had received MCT one week earlier caused lower peak pulmonary pressure and less RV hypertrophy [14]. Even if EPCs were injected into the lungs of dogs with

147

MCT-induced PAH, pulmonary artery pressure and pulmonary vascular resistance decreased and cardiac output increased [15].

To develop a therapeutic strategy in which a patient with developed PAH will be treated by i.v. administration of autologous bone marrow-derived MSCs, we investigated whether rats with MCT-induced PAH are treated successfully after i.v. administration of bone marrow-derived MSCs isolated from rats with MCT-induced PAH. As a reference cell type we chose skin fibroblasts (SFs) of healthy rats, used by Zhao *et al.* [12] to distinguish between stem cells and differentiated cells in terms of therapeutic effect of rats with PAH.

To analyse the effects of MCT-induced PAH and cell therapy in this model, we measured (*i*) RV pressures, (*ii*) RV volumes and RV ejection fraction, (*iii*) RV hypertrophy, (*iv*) expression of genes associated with myocardial hypertrophy, such as β-myosin heavy chain, pro-atrial natriuretic peptide and pro-B-type natriuretic peptide, (*v*) RV myocardial expression of tenascin-C and collagens I and III, and (*vi*) RV myocardial concentrations of collagenolytic enzymes, such as matrix metalloproteinase-1 (MMP1), cathepsin K and cathepsin S, in normal rat hearts and in hearts of rats with MCT-induced PAH without and with cell therapy.

Materials and Methods

Animal model

All animals were treated in accordance with the national guidelines and with permission of the Animal Experiments Committee of the Leiden University Medical Center. Healthy, adult, female Wistar rats (200-250 g body weight; Harlan, Zeist, the Netherlands) were randomly assigned to four experimental groups. At day 1, group 1 received subcutaneous (s.c.) PBS (Control, n=10), the other groups received a single s.c. injection of MCT (Sigma-Aldrich, Zwijndrecht, the Netherlands; 60 mg/kg, n=10 each group). At day 14, group 1 and 2 received 1 ml PBS intravenously (i.v.), rats from group 3 were treated by i.v. administration of 10^6 MSCs, whereas rats from group 4 received 10^6 skin fibroblasts (SFs). The animals were housed, two animals per cage, with a 12h/12h light/dark cycle and an unrestricted food supply. The rats were weighed three times per week.

Mesenchymal stem cell isolation and culture

To obtain MSCs, donor rats were injected s.c. with MCT (60 mg/kg, n=5) and anaesthetized with isoflurane and killed by i.v. injection of KCl (100 mmol/L) after 28 days. Femurs and tibiae were removed and cleaned of all connective tissue and attached muscle. The proximal ends were clipped and bones placed in microfuge tubes supported by plastic inserts cut from pipette tips. Microfuge tubes were briefly centrifugated at 13,000 rpm for 1 min. The marrow pellets were resuspended in 10 mL of growth medium [Dulbecco Minimal Essential Medium (DMEM) supplemented with 15% fetal bovine serum (FBS; Invitrogen, Breda, the Netherlands), penicillin (50 U/L), streptomycin (50 μg/L), and amphothericin B solution (0.25 μg/mL, Sigma-Aldrich)] supplemented with 6% heparin (400 IE/ml). This suspension was centrifuged again at 1000 rpm for 10 min. Next, the pellet

was resuspended in 7 mL of growth medium supplemented with 5.75 µg/mL DNase I (Sigma-Aldrich). The cells were plated in a 25-cm^2 culture flasks (Becton Dickinson, Franklin Lakes, NJ, USA) and the culture was kept in a humidified hypoxic incubator CO_2/O_2 (5%/5%) at 37°C. The non-adherent cells were replated after 6 h. Two days later, non-adherent cells were removed by changing the medium to 12 mL of fresh growth medium. The medium was refreshed twice a week until the primary cultures were confluent. Previously it was reported that MSCs cultured in 2%-5% O_2 have increased proliferation rate and upregulated VEGF expression compared to MSCs cultured in ambient air, while maintaining their multi-lineage potential [16-20]. As far as differentiation capacity of MSCs is concerned, hypoxia was shown to have positive [16] as well as negative effects on osteogenic differentiation [19,21-23].

Before injection, the cells were trypsinized and labelled with the viable fluorescent dye CM-DiI according to the manufacturer's recommendations (CellTracker™, Molecular Probes, Invitrogen).

In vitro assays of MSCs

MSCs from MCT-treated rats and healthy rats, grown in hypoxic or normoxic incubator were tested for (***i***) proliferation rate, (***ii***) membrane protein repertoire by FACS, (***iii***) production and secretion of VEGF, and (***iv***) capacity of adipogenic and osteogenic differentiation. In addition, it was tested what effects the major metabolite of MCT, dehydromonocrotaline (dhMCT), has on proliferation and VEGF production/secretion by MSCs, by incubation of MCSs with dhMCT *in vitro*.

Proliferation rate of MSCs

MSCs isolated from bone marrow of healthy rats and bone marrow of rats with MCT-induced PAH were grown at 5% oxygen and at 20% oxygen in 96-well plates. At two moments in time, spaced 4 days, media were poured off, and cells were analysed with the XTT assay (Roche, Almere, the Netherlands). The assay is based on the cleavage of the tetrazolium salt XTT in the presence of an electron-coupling reagent, producing a soluble formazan salt. This conversion only occurs in viable cells. The measured absorbance directly correlates to the cell number.

Flow cytometry of MSCs

MSCs isolated from bone marrow of healthy rats and bone marrow of rats with MCT-induced PAH were grown in 5% oxygen and 20% oxygen incubators, and analysed for surface marker expression by flow cytometry. The MSCs were detached using trypsin/EDTA (Bio-Whittaker Europe, Verviers, Belgium) and resuspended in PBS containing 0.5% bovine serum albumine (Sigma-Aldrich), and divided in aliquots of 5×10^4 cells. Cells were then incubated for 30 min at 4°C with fluorescein isothiocyanate (FITC)- or phycoerythrin (PE)-conjugated antibodies against rat CD34, CD29, CD44, CD45, CD106 (all from Becton Dickinson) and CD90 (Serotec, Kidlington, Oxford, UK). Labeled cells were washed and analyzed using a FACSort flow cytometer (BD Pharmingen, San Jose, CA, USA), equipped with a 488-nm argon ion laser and a 635-nm red diode laser. Isotype-matched control antibodies (BD Pharmingen) were used to

determine background fluorescence. At least 5000 cells per sample were acquired and data were processed using CellQuest software (BD Pharmingen). Generally, MSCs are found to be positive for CD29, CD44, CD90 CD105 and CD106, and negative for CD34 and CD45 (unpublished observations).

Production and secretion of VEGF by MSCs

MSCs isolated from bone marrow of healthy rats and bone marrow of rats with MCT-induced PAH were grown at 5% oxygen in 96-well plates. At two moments in time, spaced 4 days, media were poured off, and cells were analysed for protein content using the bicinchonic acid (BCA) protein assay (Pierce, Etten-Leur, the Netherlands). The media were assayed for VEGF using a rat VEGF assay kit (rat base kit supplied with rat VEGF microparticle concentrate, R&D Systems Europe, Abingdon, UK). VEGF concentrations in the media were expressed as ng per mg of cellular protein.

Adipogenic and osteogenic differentiation of MSCs

MSCs isolated from bone marrow of healthy rats and bone marrow of rats with MCT-induced PAH grown in a 5% oxygen incubator were characterized using established differentiation assays [24]. Briefly, 5000 MSCs per well were plated in a 12-well culture plate, and exposed to adipogenic or osteogenic induction medium. Adipogenic differentiation medium consisted of a regular culture medium (DMEM supplemented with 15% FBS, 100 U/L penicillin and 100 µg/mL streptomycin, 1 µg/mL amphothericin B solution) supplemented with 5 µg/mL insulin, 1 µmol/L dexamethason, 50 µmol/L indomethacin and 0.5 µmol/L 3-isobutyl-1-methylxanthine (IBMX) (all from Sigma-Aldrich), and was refreshed every 3-4 days for a period of 3 weeks. Lipid accumulation was assessed by Oil Red O staining of the cultures (15 mg Oil Red O/mL of 60% isopropanol) and light microscopy. Osteogenic differentiation medium consisted of culture medium supplemented with 10 mmol/L β-glycerophosphate, 50 µg/mL ascorbic acid and 10 nmol/L dexamethason (all from Sigma-Aldrich), and was refreshed every 3-4 days for a period of 2 weeks. Afterwards, the cells were washed with phosphate-buffered saline (PBS), and calcium deposits were visualized by staining of the cells for 2-5 min with 2% Alizarine Red S in 0.5% NH_4OH (pH 5.5).

Effects of dehydroMCT on MSCs in vitro

Dehydromonocrotaline (dehydroMCT) was prepared from MCT by chemical oxidation using o-chloranil according to Mattocks *et al.* [25]. Mass spectrometric analyses have shown that 25-30% of the input MCT was converted to dehydroMCT by this method [26]. Proliferation of MSCs from healthy rats in the absence and presence of 50 µmol/L dehydroMCT was determined by XTT assay (Roche) over a 4-day interval.

Skin fibroblasts

Skin fibroblasts (SFs) were grown from pieces of skin of healthy rats anesthetized by CO_2 and killed by i.v. injection of KCl (100 mmol/L). Skin samples were transferred to porcine gelatin (Sigma-Aldrich)-coated flasks, and cultured in DMEM containing 100 U/mL penicillin, 100 µg/mL streptomycin, and 10% FBS (all

from Invitrogen) in a normoxic incubator (20% O_2 and 5% CO_2) at 37°C. Outgrowth of cells was visible 2 days after culture initiation. Three days later the skin pieces were removed and the skin fibroblasts were detached with trypsin-EDTA solution (Invitrogen), and reseeded in new culture flasks.

For intravenous infusion into rats which had had MCT administration 14 days earlier, we used passage 4-6. Prior to injection into the jugular vein, the SFs were labeled with a DiI derivative according to the recommendations of the supplier (CellTracker CM-DiI, Molecular Probes, Invitrogen). Per rat, 10^6 SFs in 0.5 mL of PBS were injected in the jugular vein.

Cell injection

At day 14, the rats were anaesthetized with isoflurane, the left jugular vein was cannulated (20G, Biovalve, Vygon, Ecouen, France), and 1 mL of cell suspension (10^6 cells/mL) or an equal amount of PBS (control animals) was injected slowly in approximately 30 s. The cell suspensions contained either MSCs from rats with MCT-induced PAH or SFs from healthy rats. Next, the canula was removed, the vein was pressed for 5 min to ensure closure of the puncture, and the skin was closed.

Hemodynamic measurements

RV function was measured as published previously [4]. Briefly, the rats were sedated by inhalation of a mixture of isoflurane (4%) and oxygen. Subsequently, general anesthesia was induced by intraperitoneal (i.p.) injection of a fentanyl—fluanison–midazolam mixture in a dose of 0.25 mL/100 g body weight. The mixture consisted of two parts Hypnorm (0.315 mg/mL fentanyl+10 mg/mL fluanison; Vital-Pharma, Maarheeze, the Netherlands): one part Dormicum (5 mg/mL midazolam; Roche, Mijdrecht, the Netherlands) and one part saline. The animals were placed on a controlled warming pad to keep body temperature constant. A tracheotomy was performed, a cannula (18G, Biovalve) was inserted, and the animals were mechanically ventilated using a pressure-controlled respirator and a mixture of air and oxygen. The animals were placed under a stereomicroscope (Zeiss, Hamburg, Germany), and the left jugular vein was cannulated for infusion of hypertonic saline (10%) to determine parallel conductance. A midsternal thoracotomy was performed, and a combined pressure-conductance catheter (model FT212, SciSense, London, Ontario, Canada) was introduced via the apex into the RV and positioned towards the pulmonary valve. The catheter was connected to a signal processor (FV898 Control Box, SciSense) and RV pressures and volumes were recorded digitally. All data were acquired at a sample rate of 2,000 Hz and analyzed off-line by dedicated software. The slope factor α was calculated as the cardiac output determined by the uncalibrated conductance catheter divided by the cardiac output determined by LV echocardiography (VisualSonics, Toronto, Ontario, Canada).

Hemodynamics

Heart rate, stroke volume, cardiac output, RV end-diastolic volume, RV end-systolic volume, RV ejection fraction, RV end-diastolic pressure, RV end-systolic

pressure, and RV peak-systolic pressure were determined from steady state pressure-volume loops. In addition, stroke work (SW) was obtained as the area of the pressure-volume loop, and the maximal rates of RV pressure upstroke and fall (dP/dt_{max} and dP/dt_{min}, respectively) were calculated. The relaxation time constant (τ) was assessed as the time constant of monoexponential decay of RV pressure during isovolumic relaxation [27]. Effective pulmonary arterial elastance (E_a), as a measure of RV afterload, was calculated as RV end-systolic pressure divided by RV stroke volume.

RV end-systolic and end-diastolic pressure-volume relations (ESPVR and EDPVR) and the preload recruitable stroke work relation (PRSW: RV-stroke work vs. RV end-diastolic volume) were determined from pressure-volume loops recorded during transient preload reduction by occlusion of the inferior vena cava. End-systolic elastance E_{es}, the linear slope of the ESPVR, and M_w, the slope of the PRSW, are load-independent measures of systolic ventricular function. Diastolic stiffness was determined as the slope of the EDPVR, E_{ed} [28].

Tissue preparations

After hemodynamic measurements heart and lungs were taken out. From each heart the ventricles were isolated, the RV was cut free, and the remainder was split into the intraventricular septum (IVS) and the left ventricle (LV). These three parts of ventricular tissue were weighed, and each was split in three parts for individual storage (*i*) at -80°C for RNA isolation, (*ii*) at -80°C to prepare homogenates, and (*iii*) in formaline (4%) to perform histochemical analysis.

Assessment of RV hypertrophy

As an indicator of right ventricular hypertrophy the weight ratio of RV/(LV + IVS) was calculated. Independently, we determined the length and width of 25-50 cardiomyocytes per group (control, MCT60, MCT+MSC and MCT+SF) isolated from the RV and LV of collagenase-dissociated hearts.

Real-time RT-PCR

Total RNA was isolated from heart tissue homogenates using guanidium-phenol-chloroform extraction and isopropanol precipitation (RNA-Bee, Tel-Test Inc., Bio-Connect BV, Huissen, the Netherlands). The RNA sample was dissolved in RNase-free water and quantified spectrophotometrically. The integrity of the RNA was studied by gel electrophoresis on a 1% agarose gel, containing ethidium bromide. Samples did not show degradation of ribosomal RNA by visual inspection under ultraviolet light. First-strand cDNA synthesis was performed with the SuperScript Choice System (Life Technologies, Breda, the Netherlands) by mixing 2 µg total RNA with 0.5 µg of oligo(dT)12-18 primer in a total volume of 12 µL. After the mixture was heated at 70°C for 10 min, a solution containing 50 mmol/L Tris·HCl (pH 8.3), 75 mmol/L KCl, 3 mmol/L $MgCl_2$, 10 mmol/L DTT, 0.5 mmol/L dNTPs, 0.5 µL RNase inhibitor, and 200 U Superscript Reverse Transcriptase was added, resulting in a total volume of 20.5 µL. This mixture was incubated at 42°C for 1 h; total volume was adjusted to 100 µL with RNase-free water and stored at –80°C until further use. For real-time quantitative PCR, 1 µL

of first-strand cDNA diluted 1:10 in RNase-free water was used in a total volume of 25 µL, containing 12.5 µL 2x SYBR Green PCR Master Mix (Applied Biosystems, Foster City, CA, USA) and 200 ng of each primer.

Primers, designed with the Primer Express software package (Applied Biosystems), were:

Primers (orientation: 5'-3')

	Forward	reverse
proANP	CCAGGCCATATTGGAGCAAA	AGGTTCTTGAAATCCATCAGATCTG
proBNP	GAAGCTGCTGGAGCTGATAAGAG	TGTAGGGCCTTGGTCCTTTG
α-MHC	CTTCAAGCTCAAGAATGCCTATGA	TGCACATTTTTACCCCCTTCTC
β-MHC	AGGCCCAGAAACAAGTGAAGAG	GGCACGGACTGCGTCATC
β-actin	GGCTCCTAGCACCATGAAGATC	GAGCCACCAATCCACACAGA

PCR reactions, consisting of 95°C for 10 min (1 cycle), 94°C for 15 s, and 60°C for 1 min (40 cycles), were performed on an ABI Prism 7900 HT Fast Real Time PCR system (Applied Biosystems). Data were analyzed with the ABI Prism 7900 sequence detection system software (version 2.2) and quantified with the comparative threshold cycle method with β-actin as a housekeeping gene reference [29].

(Immuno)histochemistry

After fixation, heart tissue samples were embedded in paraffin. Blocks were embedded in upright position to distinguish the endocardium, the midwall, and the epicardium of the RV and LV free wall in cross-sections. Tissue was cut into 4-µm thick sections and dried for at least 24 h at 37°C. After 10 min incubation at 60°C, sections were deparafinized in Ultraclear (Klinipath, Duiven, the Netherlands) for 5 min and rehydrated in decreasing graded alcohols (100-25%) followed by two 5-min washes in distilled water and TBS (150 mmol/L NaCl, 10 mmol/L Tris-HCl, pH 8.0).

To study the distribution of myocardial collagen I, collagen III, and tenascin-C, sections were exposed to immunohistochemistry. Inhibition of endogenous peroxidase activity was obtained by 20 min incubation in 0.3% hydrogen peroxide in PBS. The sections were incubated in citrate buffer at 97°C for 10 min, to retrieve antigens and subsequently washed in PBS, 5 times for 3 min, and in PBS-Tween for 2 times. Sections were incubated for 3h at room temperature with (*i*) rabbit anti-collagen I antibody (1:200; ab24133, Abcam, Cambridge, UK), (*ii*) rabbit anti-collagen III antibody (1:200; ab7778, Abcam), and (*iii*) rabbit anti-tenascin-C antibody (1:200; sc20932, Santa Cruz Biotechnology, Santa Cruz, CA, USA), followed by goat anti-rabbit IgG conjugated to HRP (1:200, sc3837, Santa Cruz Biotechnology). After series of three washes in PBS and once in PBS-Tween, 1% BSA, and 0.05% Tween, the slides were developed with diaminobenzidine (DAB) solution (Pierce, Perbio Science, Etten-leur, the Netherlands). Nuclei were counterstained using hematoxylin for 2 min, followed by dehydration with graded alcohols and clearance in xylene. Finally, the sections were mounted with D.P.X. (BDH, VWR International, Lutterworth, Leicestershire, UK), covered with glass cover slips, and examined in a light microscope (Nikon

Eclipse, Nikon Europe, Badhoevedorp, the Netherlands) equipped with a digital camera (Nikon DXM 1800). Images were analyzed using Image-Pro Plus software (Media Cybernetics, Silver Spring, MD, USA). Per section, at least 16 images were acquired and analyzed to compensate for variations within a section.

Western blotting

Myocardial samples for biochemical analysis were freeze-dried, and homogenized in homogenising buffer (0.1 M Tris-HCl and 0.1% (v/v) Tween-20, pH 7.5), using a Potter tube (Kimble/Kontes, Vineland, NJ, USA). Homogenates (1 %, $^w/_v$) were stored in aliquots at -80°C. Protein concentrations were determined by bicinchoninic acid protein (BCA) assay (Pierce, Etten-Leur, the Netherlands).

For western blot analysis the heart homogenate were separated on a 12% Bis-Tris NuPage gel (Invitrogen) and blotted on a PVDF membrane (GE Healthcare, Diegem, Belgium). Non-specific binding sites were blocked by incubating the membranes in a blocking solution 20 g/L ECL Advance Blocking Agent (GE Healthcare) in TBS-Tween (10 mmol/L Tris-HCl, pH 8.0, 150 mmol/L NaCl, 0.05% Tween) for 1 h on an orbital shaker. Subsequently, membranes were incubated with (***i***) rabbit anti-MMP1 antibody conjugated to HRP (1:20,000, ab53142, Abcam), (***ii***) goat anti-cathepsin S antibody (1:20,000, sc6503, Santa Cruz Biotechnology) followed by donkey anti-goat IgG conjugated to HRP (1:10,000, sc2020, Santa Cruz Biotechnology), and (***iii***) rabbit anti-cathepsin K antibody (1:20,000, #3588-100, BioVision, Mountain View, CA, USA) followed by goat anti-rabbit IgG conjugated to HRP (1:10,000, sc3837, Santa Cruz Biotechnology). Subsequently, the membranes were washed four times in TBS-Tween, and incubated with a chemiluminescent reagent (ECL Advance kit, GE Healthcare) for 5 min. Light emission was detected by exposure to Hyperfilm ECL (GE Healthcare). The Western blot band intensities were quantified by the Molecular Imager ChemiDoc XRS system (Bio-Rad, Veenendaal, the Netherlands).

Cardiomyocyte isolation

A separate series of 20 rats were given the same experimental treatments (n=5 per group) as mentioned earlier. At day 28, the rats were anaesthetised and the thorax was opened. The heart was taken out quickly and immediately put into ice-cold, oxygenated Tyrode solution. The aorta was connected to the cannula of a Langendorff perfusion set-up (AD Instruments, Spechbach, Germany). The heart was perfused for 5 min with an oxygenated Tyrode solution at constant pressure (70 mmHg) at 37° C and resumed beating. The perfusion fluid was replaced by an oxygenated, low Ca^{2+} perfusion fluid. Contractions disappeared within 30 s. After 5 min of low calcium perfusion, the perfusion was continued in a recirculating manner at a perfusion pressure of ~60 mm Hg. At that time collagenase (0.06%, Worthington, Lakewood, NJ, USA) was added. Thirty min later, the flow rate was too high to maintain a perfusion pressure of 60 mm Hg. Then, the heart was removed, and the RV was separated from the LV (including IVS) using a scalpel. RV and LV were cut in small pieces, incubated in a fresh collagenase (0.06%) solution, and dissociated in a waterbath shaker at 37ºC. Thereafter, sedimented cardiomyocytes were resuspended and stored at 37ºC in fresh HEPES-buffered

154

salt solution containing (in mmol/L) NaCl 125, KCl 5, $MgSO_4$ 1, KH_2PO_4 1, $CaCl_2$ 1.8, $NaHCO_3$ 10, HEPES 20, glucose 5.5, pH 7.4. The average fraction of rod-shaped cardiomyocytes was 80%. The percentage of rod-shaped cardiomyocytes decreased by about 10% during 6 h at 37° C. Per heart, roughly 50 intact, non-contracting, rod-shaped cardiomyocytes from RV as well as LV were photographed followed by measurement of length and width with calibrated ruler.

Statistical analysis

To assess the effect of treatment (cell therapy with MSCs, cell therapy with SFs vs. treatment by PBS) differences between groups were evaluated by one-way ANOVA followed by Bonferroni's *post-hoc* test (SPSS12 for Windows, SPSS Inc., Chicago, IL, USA). Differences were considered significant at p<0.05. Values are represented by means ± SD, unless stated otherwise.

Results

Proliferation rate of MSCs

MSCs from healthy rats proliferated roughly 2 times more rapidly than MSCs from MCT-treated rats if grown at 5% oxygen (p=0.028) but if grown at 21% oxygen this difference was absent (p=0.576). The use of an incubator with 5% oxygen was associated with higher proliferation rates of MSCs than in case using 21% oxygen, whether they originated from healthy rats or MCT-treated rats (≈3-fold, p=0.007 and ≈2-fold, p=0.061, respectively) (Figure 1, top left panel).
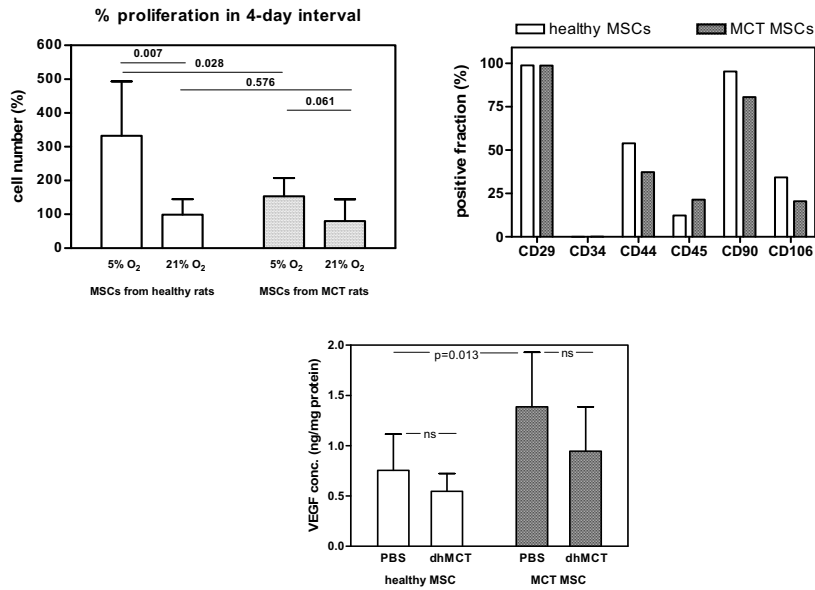

Figure 1. Top left panel. Proliferation of MSCs in 4-day intervals. MSCs from healthy rats and MSCs from rats with MCT-induced PAH were grown in an incubator with 5% oxygen, 5% CO2 and 90% nitrogen (5% O2) or in an incubator with 5% CO2 and air (21% O2). If grown in 5% oxygen, MSCs from healthy rats proliferated ≈2 times more rapidly than MSCs from rats with MCT-induced PAH (p=0.028), but if grown in 21% oxygen, proliferation rate did not differ between the two groups of MSCs (p=0.576).
Top right panel. Surface marker profile of MSCs from bone marrow of healthy rats and of MSCs from bone marrow of rats with MCT-induced PAH. Both types of MSCs were cultured in a 5% O2/5% CO2 incubator.
Bottom panel. VEGF concentration in the culture medium of MSCs isolated from healthy rats (healthy MSC) and isolated from rats with MCT-induced PAH. The stem cells were grown for 4 days in culture medium. After that time medium and cells were split, medium was analyzed for VEGF concentration, and cells were analyzed for protein content. Medium VEGF concentration is expressed as pg of VEGF in the medium per mg of cellular protein.

FACS analysis of MSCs

Comparison of FACS data obtained from MSCs isolated from rats with MCT-induced PAH with those obtained from MSCs from healthy rats, revealed minor differences in the repertoire of surface markers (Figure 1, top right). Both types of MSCs were cultured in a 5% O_2/5% CO_2 incubator.

VEGF production and secretion from MSCs

MSCs from healthy rats and MSCs of rats with MCT-induced PAH were grown in an 5% O_2/5% CO_2 incubator in 96-well plates for 4 days. At t=0 and t=4 days media were analysed for VEGF concentration, and cells were analysed for protein content. MSCs from rats with MCT-induced PAH had $\approx$2-fold higher VEGF secretion than MSCs from healthy rats (p<0.02) (Figure 1, bottom panel). Addition of 50 µmol/L of dehydroMCT, the toxic metabolite of MCT, slightly depressed VEGF secretion from both types of MSCs, but these decreases were not significant.

Differentiation potential of MSCs

MSCs from healthy rats and from rats with MCT-induced PAH, grown in a 5% O_2/5% CO_2 incubator, were investigated for adipogenic and osteogenic differentiation capacity. Adipogenic and osteogenic differentiation capacities, present in MSCs obtained from healthy rats, were well preserved in MSCs obtained from MCT-treated rats (Figure 2).
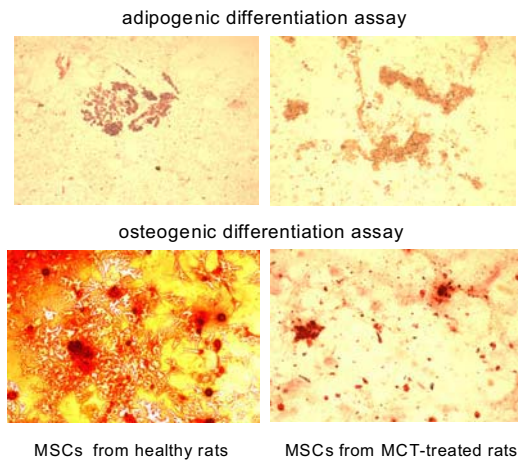
adipogenic differentiation assay

osteogenic differentiation assay

MSCs from healthy rats   MSCs from MCT-treated rats

Figure 2. Differentiation into adipogenic phenotype (upper panels) and osteogenic phenotype (bottom panels) of MSCs isolated from healthy rats (left panels) and isolated from rats with MCT-induced PAH (right panels).

157

Body weights

The rats were weighed 3 times per week. The net body weight gain of rats with MCT-induced PAH in 4 weeks was less than that of control rats (18.1±6.9 g vs. 28.1±8.2 g, p<0.05). The body weight gain in the MCT+MSC group was 20.6± 8.2 g, which was not significantly different from the MCT60 group, nor from the control group. The body weight gain in the MCT+SFB group was 17.9±8.1 g (n.s. vs. MCT60; p<0.05 vs. control) (Figure 3).
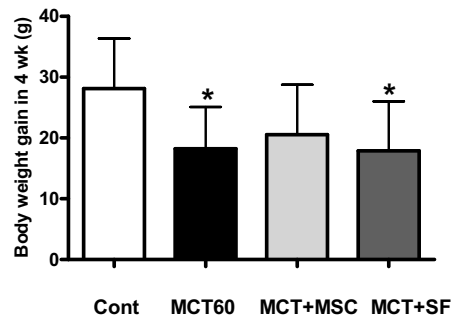

Figure 3. Increase in body weight in 4 weeks of the 4 groups of rats (control, MCT60, MCT+MSC and MCT+SFBs). Indicated are mean values ± SD. (* p<0.05 vs. Control, # p<0.05 vs. MCT60).

RV peak systolic pressure

At the end of the experimental period, RV peak systolic pressures were significantly higher in MCT group than in the control group, indicating the development of PAH (41.5±16.9 vs. 27.2±4.9 mmHg in control; p<0.05). If MCT-treated rats had been given cell therapy with MSCs, mean RV peak systolic pressure was attenuated (30.7±4.4 mmHg) although not significantly (p=0.08 vs. MCT60; n.s. vs. control). If MCT-treated rats had been given cell therapy with SFBs, mean RV peak systolic pressure was 32.1±5.7 mmHg (n.s. vs. MCT60; n.s. vs. control) (Figure 4a).

RV function

Consistent with previous studies, MCT induced PAH and changes in RV volumes and ejection fraction. The hemodynamic effects are evident from the significant differences between the Control group and the MCT60 group: RV ejection fraction decreased, whereas RV peak pressure, RV end-systolic volume and RV end-diastolic pressure all increased (Table 2).

Table 2. Hemodynamic data of the rats that have been treated without or with MCT, and with and without additional cell therapy using MSCs or SFs. Data is collected at 28 days after MCT (or control) treatment.

		Control	**MCT60**	**MCT+MSC**	**MCT+SF**
Right Ventricle					
Heart rate	HR (bpm)	330±26	341±36	327±26	348±26
Stroke volume	SV (µL)	228±50	234±64	287±37	259±29
Cardiac output	CO (mL/min)	74±13	79±20	93±10*	90±9
Ejection fraction	EF (%)	56.2±11.2	42.8±6.2*	52.1±5.2	49.1±11.1
End-systolic volume	ESV (µL)	200±103	323±132	270±75	295±118
End-diastolic volume	EDV (µL)	427±150	556±183	557±99	554±143
End-systolic pressure	ESP (mmHg)	24±5	38±15*	28±4	30±5
End-diastolic pressure	EDP (mmHg)	1.3±1.2	3.9±1.8*	1.9±0.9	2.9±2.0
Peak pressure	Pmax (mmHg)	27.2±4.9	41.5±16.9*	30.7±4.4	32.1±5.7
dP/dt max	dPdtMax (mmHg/s)	1565±383	2215±1040	1832±455	1916±389
Negative dP/dt min	-dPdtMin (mmHg/s)	1334±385	1912±860	1675±493	1551±252
Stroke work	SW (mmHg.µL)	5071±1415	7044±2238	6682±1117	6239±1415
Relaxation time constant	Tau (ms)	13.7±3.8	14.0±2.9	12.9±4.7	13.5±4.7
Arterial elastance (afterload)	Ea (mmHg/µL)	0.11±0.04	0.19±0.12	0.10±0.03[#]	0.12±0.03
End-systolic elastance	Ees (mmHg/µL)	0.19±0.17	0.17±0.20	0.10±0.07	0.12±0.07
End-diastolic elastance	Eed (mmHg/µL)	0.008±0.005	0.010±0.004	0.007±0.004	0.009±0.003
Preload recruitable stroke work	PRSW (mmHg)	21±7	25±15	19±5	23±7

* *p*-value < 0.05 vs. Cont
[#] *p*-value < 0.05 vs. MCT60

The animals that received MCT and were subsequently treated with MSCs showed much less pronounced differences in pressure and volume compared to the Control group. This indicates that MSC treatment substantially modified the effects of MCT. Compared to the MCT60 group, the MCT+MSC group showed

higher RV ejection fraction (Fig. 4b), higher stroke volume, and lower RV end-diastolic pressure, although these changes did not reach statistical significance. The MCT-induced changes in RV end-systolic and end-diastolic volumes, including the effects of i.v. therapy with MSCs and SFs are shown in Fig. 4c and d.
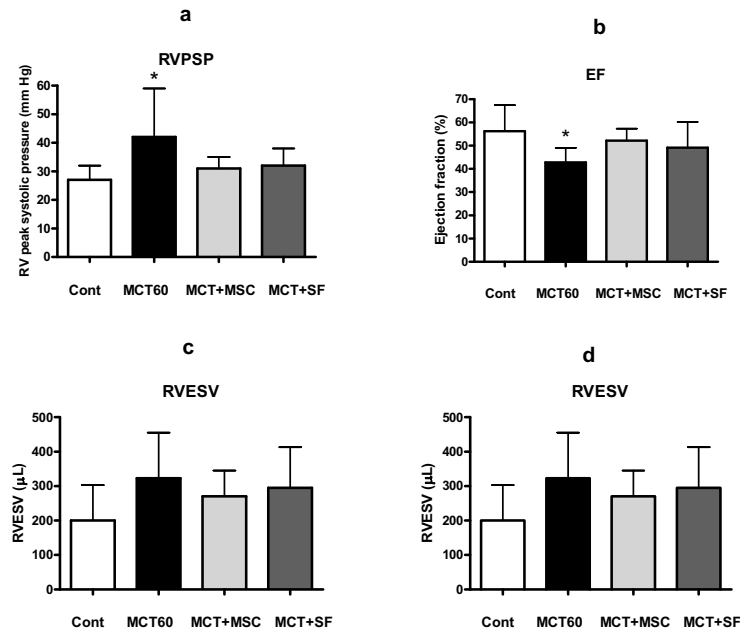

Figure 4a. RV peak systolic pressures, **b.** Ejection fraction (EF), **c.** RV end-systolic volumes (RVESV), and **d.** RV end-diastolic volumes (RVEDV) of the 4 groups of rats (control, MCT60, MCT+MSC and MCT+SFB). Indicated are mean values ± SD (* p<0.05 vs. Control).

Right ventricular hypertrophy

As a measure of RV hypertrophy we calculated the weight ratio of RV/ (LV+IVS). At 28 days after MCT, rats had developed RV hypertrophy with a RV/ (IVS+LV) weight ratio of 0.47±0.12 vs. 0.25±0.04 in control rats (p<0.001). In PAH rats treated with MSCs, RV/ (IVS+LV) weight ratio was near normal (0.32±0.07; p<0.005 vs. MCT60; n.s. vs. control). In PAH rats treated with SFBs, RV/ (IVS+LV) weight ratio was 0.35±0.06 (p<0.05 vs. MCT60; n.s. vs. control (Figure 5).
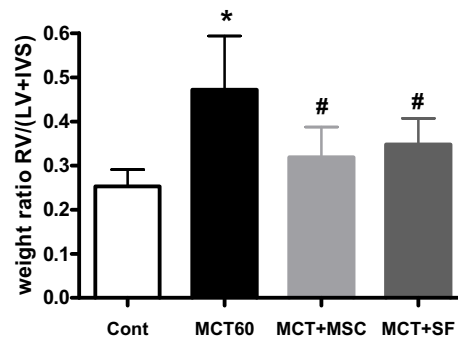
Figure 5. RV/ (LV+IVS) weight ratio of the hearts of the 4 group of rats (Control, MCT60, MCT+MSC, and MCT+SF). Indicated are mean values ± SD.

Length and width of isolated RV cardiomyocytes were increased in rats that had received MCT compared to PBS-treated rats (Table 1). Although in control hearts RV cardiomyocyte dimensions are smaller than those of LV cardiomyocytes (significant difference for cardiomyocyte width only), in MCT-treated rats RV cardiomyocyte dimensions are larger than those of LV cardiomyocytes (significant differences for both width and length). Cell therapy with MSC reduces RV cardiomyocyte dimensions to levels that do not differ from dimensions of LV cardiomyocytes. Surprisingly, also the hearts of rats that had cell therapy with SFs showed equal dimensions of RV and LV cardiomyocytes (Table 1).

Table 1. Dimensions of cardiomyocytes isolated from hearts of rats treated without or with MCT, and with and without additional cell therapy using MSCs or SFs.

	RV cardiomyocytes	LV cardiomyocytes	P RV vs LV
	mean±SD (n)	mean±SD (n)	
Cardiomyocyte length (µm)			
Control	99±19 (200)	102±20 (166)	0.087
MCT60	108±24 (221) *	100±18 (209)	**<0.001**
MCT+MSC	103±19 (201)	103±19 (232)	0.999
MCT+SFB	102±21 (204) #	103±18 (176)	0.618
Cardiomyocyte width (µm)			
Control	16.8±3.0 (200)	17.7±3.1 (166)	**0.005**
MCT60	18.2±3.0 (221) *	17.5±3.1 (209)	**0.017**
MCT+MSC	17.3±3.2 (201) #	17.8±3.2 (232)	0.106
MCT+SFB	16.9±3.2 (204) #	17.4±2.8 (176)	0.083

* *p<0.05 vs. Control*
# *p<0.05 vs. MCT60*

161

mRNA in RV myocardium

RV myocardial concentrations of mRNAs encoding ANP and BNP were increased in rats with MCT-induced PAH compared to control rats, although not significantly (Figure 6). In RV myocardium of MCT-treated rats, mRNA of αMHC increased and mRNA of βMHC decreased, although not significantly, compared to PBS-treated rats. Cell therapy with MSCs or SFBs had no significant effects on these parameters.
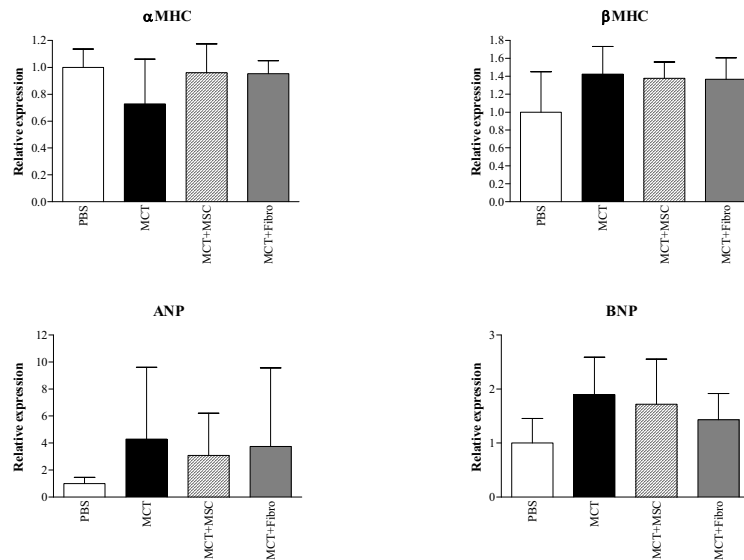

Figure 6
Right ventricular concentrations of mRNA encoding α- and β-myosin heavy chain (αMHC and βMHC, respectively), pro-atrial natriuretic peptide (ANP), and pro-B-type natriuretic peptide (BNP). Indicated are mean values ± SD.

Extracellular matrix proteins

In normal RV and LV myocardium tenascin-C concentrations are very low (figure 7). However, in RV myocardium of rats of the MCT60 group tenascin-C concentration is increased considerably (p<0.005 vs. control), whereas in the corresponding LV myocardium the tenascin-C concentrations remained low. In RV myocardium of rats from the MCT+MSC group the tenascin-C is as low as the tenascin-C concentration in the accompanying LV myocardium, which levels are not significantly different from corresponding values in control myocardium (Table 3). Myocardial collagen I and III concentrations were increased in RV myocardium of the MCT60 group, compared to the LV myocardium of the same hearts. Upon therapy with MSCs RV myocardial concentrations of collagen I and III remained elevated (both n.s. vs. MCT60), although comparison between RV and LV was only significant for collagen I.

Table 3. Myocardial concentrations of extracellular matrix proteins in RV and LV of rats that have been treated without or with MCT, and without or with additional therapy using MSCs

	Control	MCT60	MCT+MSC	$P_{MCT60\ vs\ Control}$	$P_{MCT60\ vs.\ MCT+MSC}$
Collagen I (pixels protein/total pixels)					
RV	0.072 ± 0.021	0.082 ± 0.018	0.078 ± 0.015	n.s.	n.s.
LV	0.050 ± 0.013	0.043 ± 0.020	0.034 ± 0.004	n.s.	n.s.
$P_{RV\ vs.\ LV}$	n.s.	**0.003**	**0.006**		
Collagen III (pixels protein/total pixels)					
RV	0.102 ± 0.026	0.131 ± 0.027	0.124 ± 0.026	**0.006**	n.s.
LV	0.081 ± 0.010	0.070 ± 0.021	0.095 ± 0.007	n.s.	n.s.
$P_{RV\ vs.\ LV}$	n.s.	**<0.001**	n.s.		
Tenascin-C (arbitrary units)					
RV	4475 ± 950	20138 ± 2469	6029 ± 875	**<0.001**	**<0.001**
LV	4540 ± 696	5877 ± 859	5221 ± 752		
$P_{RV\ vs.\ LV}$	n.s.	**<0.001**	n.s.		

Control   MCT60   MCT+MSC
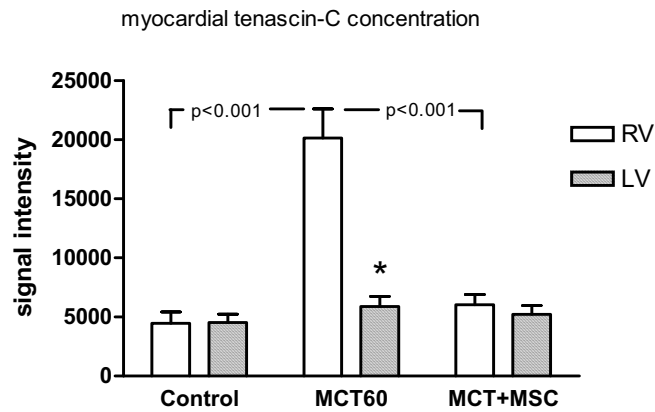
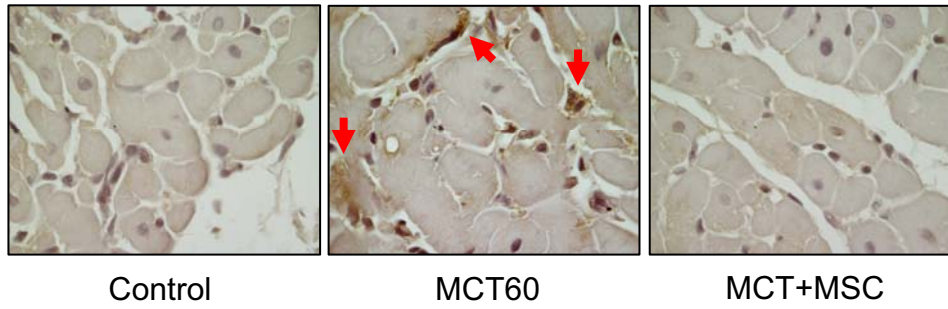myocardial tenascin-C concentration

Figure 7
Concentrations of tenascin-C in RV and LV myocardium of three groups of rats (Control, MCT60, and MCT+MSC) (lower panel). Upper panels present immunohistochemical images of myocardial tenascin-C in RV myocardium of control, MCT60 and MCT+MSC rats. Indicated are mean values ± SEM of 16-64 analyzed images.
* p<0.005 vs. RV of the same group.

Collagenase activity

To answer the question whether RV failure is associated with increased myocardial collagenase activity that would allow RV dilatation, we analyzed myocardial concentrations of MMP1, cathepsin S and cathepsin K in RV myocardium of three groups of rats (control, MCT60, and MCT+MSC). These enzymes demonstrated no significant changes in RV myocardium between the groups (Table 4). In the MCT60 group myocardial concentrations in RV and LV did not differ significantly.

Table 4. Myocardial concentrations of three collagenolytic enzymes, matrix metalloproteinase-1 (MMP1), cathepsin S and cathepsin K in RV and LV of rats that have been treated without or with MCT, and without or with additional therapy using MSCs.

	Control	MCT60	MCT+MSC	$P_{MCT60 \text{ vs}}$ Control	P_{MCT60} vs. MCT+MSC
MMP1 (pixels protein/total pixels)					
RV	1.005±0.085(4)	1.122±0.141(4)	1.121±0.192(8)	n.s.	n.s.
LV	1.098±0.185(4)	1.200±0.230(4)	1.061±0.282(8)	n.s.	n.s.
$P_{RV \text{ vs.}}$ LV	n.s.	n.s.	n.s.		
Cathepsin S (pixels protein/total pixels)					
RV	0.924±0.344(5)	0.812±0.157(4)	0.717±0.222(8)	n.s.	n.s.
Cathepsin K (pixels protein/total pixels)					
RV	1.082±0.477(4)	1.430±0.676(3)	1.340±0.571(6)	n.s.	n.s.

Discussion

In this study we showed that i.v. administration of MSCs from donor rats with PAH to acceptor rats with MCT-induced PAH decreases RV peak systolic pressure, improves RV function, and prevents RV hypertrophy, at least to a great extent.

Pulmonary hypertension often occurs as a consequence of an isolated pulmonary arteriolar vasculopathy, and then is called pulmonary artery hypertension (PAH) [1]. Increased pulmonary vascular resistance imposes an overload to the RV, ultimately leading to RV failure. Although the distribution of ventilation/perfusion relationships in PAH patients is close to normal, arterial pO_2 is usually low, as is the venous oxygen saturation [30-32]. Although administration of 60 mg/kg MCT had resulted in a significant decrease of RV ejection fraction, several biochemical markers of RV overload were not conclusively positive. Expression of βMHC, proANP and proBNP mRNA in RV myocardium of rats in the MCT60 group was increased, but not significantly different from control. On the other hand, in overloaded RV myocardium several extracellular matrix proteins, such as tenascin-C, collagen I and collagen III, showed upregulated expression, whereas RV myocardial concentrations of three collagenolytic enzymes such as MMP1, cathepsin K and cathepsin S, were not significantly changed.

Current therapies of PAH include (*i*) prostacyclin analogues [33,34] such as epoprostenol [35,36], (*ii*) calcium channel blockers [37,38], (*iii*) angiotensin-converting enzyme [39], (*iv*) endothelin receptor antagonists such as bosentan [40,41], (*v*) phosphodiesterase-5 inhibitors such as sildenafil [32,42,43], and (*vi*) lung transplantation [44].

In experimental models of PAH several groups have shown that cell therapy using bone marrow-derived endothelial-like progenitor cells [12], bone marrow-derived MSCs [14], and umbilical cord blood mononuclear cells [45] given i.v. to rats with MCT-induced PAH resulted in lower pulmonary artery pressure, less RV hypertrophy, and improved survival. Bone marrow-derived cells obtained from rats injected with 5-fluorouracil 3 days earlier were able to reverse PAH, RV hypertrophy and medial hypertrophy in pulmonary arterioles [46]. The i.v. administration of MSCs *in vitro* transduced with the endothelial nitric oxide synthase (eNOS) gene into rats with MCT-induced PAH appeared more effective than i.v. administration of unmodified MSCs [14]. Similar results have been obtained with endothelial-like progenitor cells that after i.v. injection into MCT-treated rats were more effective in reversing PAH if transduced with the eNOS gene than if unmodified [12]. Likewise, pulmonary artery-derived smooth muscle cells that have been transduced *in vitro* with the eNOS gene, administered i.v. simultaneously with MCT, prevented the development of PAH, whereas pulmonary artery-derived smooth muscle cells transduced with a control vector did not [47]. The cell type carrying the eNOS gene is apparently not important, as even fibroblasts transfected with the eNOS gene were effective in reversing established PAH [48]. These results imply a major role for NO in vasodilation and regeneration of damaged lung tissue.

To date, the only clinical study reporting i.v. cell therapy in patients with PAH is a randomized study by Wang and coworkers who described a significant improvement of 6-minute hall walk distance after i.v. administration of autologous

endothelial progenitor cells in comparison with conventional therapy [11]. Other routes of administration of cells leading to successful therapeutic effects of cell therapy on PAH include intratracheal administration [49] and intra-parenchymal injection [15].

To mimic a therapeutic strategy in which a patient with PAH is treated by i.v. administration of autologous bone marrow-derived MSCs, we used MSCs that have been isolated from bone marrow of rats with MCT-induced PAH and injected i.v. to rats that had MCT treatment 14 days earlier. MSCs isolated from bone marrow of rats with MCT-induced PAH differed from MSCs isolated from bone marrow of healthy rats in several aspects. Proliferation rate was lower and VEGF secretion was higher, but potential of adipogenic and osteogenic differentiation and surface marker profile were not changed markedly in MSCs from rats with MCT-induced PAH, as compared to MSCs from healthy rats. In the present study we demonstrated that the therapy of rats with MCT-induced PAH with MSC from rats with MCT-induced PAH was successful, as RV systolic pressure was reduced, RV hypertrophy was reduced, and RV function was improved, compared to rats with MCT treatment without cell therapy.

The mechanism of action of i.v. cell therapy with MSCs is not yet elucidated. As to the localization of DiI-labeled MSCs in the lung, 14 days after i.v. injection of 10^6 MSCs per rat, no evidence of massive integration into arteries and bronchi have been obtained. Association and integration of MSCs with pulmonary arterioles have been noticed, but this can hardly explain the substantial therapeutic efficacy of MSCs in MCT-induced lung damage. The therapeutic actions of MSCs engrafted in injured lungs are considered to be the result of paracrine effects [50]. Particularly the secretion of cytokines and growth factors is the basis of angiogenic and reverse remodeling reactions. One important paracrine factor is VEGF that induces angiogenesis by inducing proliferation, differentiation and chemotaxis of endothelial cells [51,52]. In situations of vascular trauma cytokines and growth factors, such as VEGF, promote recruitment of endothelial (progenitor) cells to promote vascular healing and repair [53,54]. Administration of pulmonary artery-derived smooth muscle cells to rats with MCT-induced PAH had therapeutic effects only if transduced *in vitro* with the VEGF-A gene [55]. Likewise, i.v. administration of fibroblasts transfected with the VEGF-A gene were effective in reversing established PAH, whereas untransduced fibroblasts were not [48]. The relationship between pulmonary vascular remodeling and lack of VEGF is demonstrated by Fujita and coworkers who showed that in mice overexpressing TNFα development of PAH is associated with decreased VEGF mRNA in lung tissue [56]. Surprisingly, the stem cells used in the present study, the MSCs from bone-marrow of rats with MCT-induced PAH, produced even more VEGF *in vitro* than the MSCs from bone-marrow of healthy rats. This finding may explain the potent therapeutic effects of the MSCs from MCT-treated rats.

Several groups have shown that i.v. administration of pulmonary artery-derived smooth muscle cells [47], skin fibroblasts [12] or bone marrow-derived mononuclear cells [13] to rats with MCT-induced PAH had no appreciable effect on RV systolic pressure and pulmonary artery remodeling. As a reference cell type we chose skin fibroblasts (SFs) of healthy rats, also used by Zhao *et al.* [12] to illustrate their lack of effectivity to treat PAH in MCT-treated rats. However, we have observed some beneficial effects of injected SFs from healthy rats on RV

systolic pressure, RV hypertrophy, and RV function, although these effects were less pronounced than observed with MSCs from rats with MCT-induced PAH. We could not detect i.v. injected SFs trapped in the lung and/or the RV myocardium, but any therapeutic effect of injected SFs on PAH and RV hypertrophy should be explained by paracrine effects on the pulmonary arterioles, thereby decreasing the pulmonary vascular resistance.

Conclusions

In conclusion we have found that intravenous administration of MSCs from rats with PAH to acceptor rats with MCT-induced PAH decreased PAH, prevented RV hypertrophy, and improved RV function. These results suggest that patients with PAH may be treated successfully with autologous MSCs.

Acknowledgements

References

1. Farber HW, Loscalzo J. Pulmonary arterial hypertension. N Engl J Med 2004; 351:1655-65.

2. Lalich JJ, Merkow L. Pulmonary arteritis produced in rats by feeding Crotolaria spectabilis. Lab Invest 1961;10: 744-50.

3. Meyrick B, Gamble W, Reid L. Development of *Crotalaria* pulmonary hypertension: hemodynamic and structural study. Am J Physiol Heart Circ Physiol 1980; 239: H692-H702.

4. Hessel MHM, Steendijk P, den Adel B, Schutte CI, van der Laarse A. Characterization of right ventricular function after monocrotaline-induced pulmonary hypertension in the intact rat. Am J Physiol Heart Circ Physiol 2006; 291: 2424-30.

5. Hessel HMH, Steendijk P, den Adel B, Schutte CI, van der Laarse A. Pressure overload-induced right ventricular dilatation is associated with re-expression of myocardial tenascin-C and increased plasma levels of tenascin-C (abstract). Circulation 2006;114 (suppl II):II-133.

6. Barton PJR, Birks EJ, Felkin LE, Cullen ME, Koban MU, Yacoub MH. Increased expression of extracellular matrix regulators TIMP1 and MMP1 in deteriorating heart failure. J Heart Lung Transplant 2003;22:738-44.

7. Li YY, Feng Y, McTiernan CF, Pei W, Moravec CS, Wang P, Rosenblum W, Kormos RL, Feldman AM. Downregulation of matrix metalloproteinases and reduction in collagen damage in the failing human heart after support with left ventricular assist devices. Circulation 2001;104:1147-52.

8. Bruggink AH. Reverse remodeling of the extracellular matrix in heart failure after left ventricular mechanical support. PhD Thesis, University Utrecht, 2008.

9. Campian ME, Hardziyenka M, Michel MC, Tan HL. How valid are animal models to evaluate treatments for pulmonary hypertension? Naunyn-Schmiedeberg's Arch Pharmacol 2006; 373: 391-400.

10. Passier R, Mummery C. Origin and use of embryonic and adult stem cells in differentiation and tissue repair. Cardiovasc Res 2003; 58: 324-35.

11. Wang X-X, Zhang F-R, Shang Y-P, Zhu J-H, Xie X-D, Tao Q-M, Zhu J-H, Chen J-Z. Transplantation of autologous endothelial progenitor cells may be beneficial in patients with idiopathic pulmonary arterial hypertension. J Am Coll Cardiol 2007;49:1566-71.

12. Zhao YD, Courtman DW, Deng Y, Kugathasan L, Zhang Q, Stewart DJ. Rescue of monocrotaline-induced pulmonary arterial hypertension using bone marrow-derived endothelial-like progenitor cells. Efficacy of combined cell and eNOS gene therapy in established disease. Circ Res 2005; 96: 442-50.

13. Sahara M, Sata M, Morita T, Nakamura K, Hirata Y, Nagai R. Diverse contribution of bone marrow-derived cells to vascular remodeling associated with pulmonary arterial hypertension and arterial neointimal formation. Circulation 2007;115:509-17.

14. Kanki-Harimoto S, Horimoto H, Mieno S, Kishida K, Watanabe F, Furuya E, Katsumata T. Implantation of mesenchymal stem cells overexpressing endothelial nitric oxide synthase improves right ventricular impairments caused by pulmonary hypertension. Circulation 2006;114(suppl I):I-181-I-185.

15. Takahashi M, Nakamura T, Toba T, Kajiwara N, Kato H, Shimizu Y. Transplantation of endothelial progenitor cells into the lung to alleviate pulmonary hypertension in dogs. Tissue Eng 2004;10:771-9.

16. Lennon DP, Edmison JM, Caplan AI. Cultivation of rat marrow-derived mesenchymal stem cells in reduced oxygen tension: effects on in vitro and in vivo osteochondrogenesis. J Cell Physiol 2001;187:345-55.

17. Grayson WL, Zhao F, Izadpanah R, Bunnell B, Ma T. Effects of hypoxia on human mesenchymal stem cell expansion and plasticity in SD constructs. J Cell Physiol 2006; 207: 331-9.

18. Grayson WL, Zhao F, Bunnell B, Ma T. Hypoxia enhances proliferation and tissue formation of human mesenchymal stem cells. Biochem Biophys Res Comm 2007; 358: 948-53.

19. Potier E, Ferreira E, Andriamanalijaona R, Pujol J-P, Oudina K, Logeart-Avramoglou D, Petite H. Hypoxia affects mesenchymal stromal cell osteogenic differentiation and angiogenic factor expression. Bone 2007;40:1078-87.

20. Buravkova LB, Anokhina EB. Effect of hypoxia on stromal precursors from rat bone marrow at the early stage of culturing. Bull Exp Biol Med 2007; 143: 411-3.

21. Matsuda N, Morita N, Matsuda K, Watanabe M. Proliferation and differentiation of human osteoblastic cells associated with differential activation of MAP kinases in response to epidermal growth factor, hypoxia, and mechanical stress *in vitro*. Biochem Biophys Res Comm 1998;249:350-4.

22. Park JH, Park BH, Kim HK, Park TS, Baek HS. Hypoxia decreases Runx2/Cbfa1 expression in human osteoblast-like cells. Mol Cell Endocrinol 2002;192:197-203.

23. Tuncay OC, Ho D, Barker MK. Oxygen tension regulates osteoblast function. Am J Orthod Dentofac Orthop 1994;105:457-63.

24. Pittenger MF, Mackay AM, Beck SC, Jaiswal RK, Douglas R, Mosca JD, Moorman MA, Simonetti DW, Craig S, Marshak DR. Multilineage potential of adult human mesenchymal stem cells. Science 1999; 284: 143-7.

25. Mattocks AR, Jukes R, Brown J. Simple procedures for preparing putative toxic metabolites of pyrrolizidine alkaloids. Toxicon 1989; 27: 561-7.

26. Sehgal PB, Mukhopadhyay S, Xu F, Patel K, Shah M. Dysfunction of Golgi tethers, SNAREs, and SNAPs in monocrotaline-induced pulmonary hypertension. Am J Physiol Lung Cell Mol Physiol 2007; 292: L1526-L1542.

27. Leeuwenburgh BP, Steendijk P, Helbing WA, Baan J. Indexes of diastolic RV function: load dependence and changes after chronic RV pressure overload in lambs. Am J Physiol Heart Circ Physiol 2002;282:H1350-H1358.

28. Burkhoff D, Mirsky I, Suga H. Assessment of systolic and diastolic ventricular properties via pressure–volume analysis: a guide for clinical, translational, and basic researchers. Am J Physiol Heart Circ Physiol 2005; 289: H501–H512.

29. Pfaffl MW. A new mathematical model for relative quantification in real-time RT-PCR. Nucleic Acids Res 2001;29: e45.

30. Dantzker DR, Bower JS. Mechanisms of gas exchange abnormality in patients with chronic obliterative pulmonary vascular disease. J Clin Invest 1979;64:1050-5.

31. Melot C, Naeije R, Mols P, Vandenbossche JL, Denolin H. Effects of nifedipine on ventilation/perfusion matching in primary pulmonary hypertension. Chest 1983;83:203-7.

32. Schermuly RT, Kreisselmeier KP, Ghofrani HA, Yilmaz H, Butrous G, Ermert L, Ermert M, Weissmann N, Rose F, Guenther A, Walmrath D, Seeger W, Grimminger F. Chronic sildenafil treatment inhibits monocrotaline-induced pulmonary hypertension in rats. Am J Respir Crit Care Med. 2004;169:39-45.

33. McLaughlin VV, Rich S. Pulmonary hypertension – advances in medical and surgical intervention. J Heart Lung Transplant 1998;17:739-43.

34. Wanstall JC, Jefferey TK. Recognition and management of pulmonary hypertension. Drugs 1998;56:989-1007.

35. Hinderliter AL, Willis PW, Barst RJ, Rich S, Rubin LJ, Badesch DB, Groves BM, McGoon MD, Tapson VF, Bourge RC, Brundage BH, Koerner SK, Langleben D, Keller CA, Murali S, Uretsky BF, Koch G, Li S, Clayton LM, Jöbsis MM, Blackburn SD jr, Crow JW, Long WA, for the Primary Pulmonary Hypertension Study Group. Effects of long-term infusion of prostacyclin (Epoprostenol) on echocardiographic measures of right ventricular structure and function in primary pulmonary hypertension. Circulation 1997;95:1479-86.

36. Oikawa M, Kagaya Y, Otani H, Sakuma M, Demachi J, Suzuki J, Takahashi T, Nawata J, Ido T, Watanabe J, Shirato K. Increased [^{18}F]fluorodeoxyglucose accumulation in right ventricular free wall in patients with pulmonary hypertension and the effect of Epoprostenol. J Am Coll Cardiol 2005;45:1849-55.

37. Sitbon O, Humbert M, Jaïs X, Ioos V, Hamid AM, Provencher S, Garcia G, Parent F, Hervé P, Simonneau G. Long-term response to calcium channel blockers in idiopathic pulmonary arterial hypertension. Circulation 2005;111:3105-11.

38. Mawatari E, Hongo M, Sakai A, Terasawa F, Takahashi M, Yazaki Y, Kinoshita O, Ikeda U. Amlodipine prevents monocrotaline-induced pulmonary arterial hypertension and prolongs survival in rats independent of blood pressure lowering. Clin Exp Pharmacol Physiol 2007;34:594-600.

39. Abraham WT, Raynolds MV, Gottschall B, Badesch DB, Wynne KM, Groves BM, Lowes BD, Bristow MR, Perryman MB, Voelkel NF. Importance of angiotensin-converting enzyme in pulmonary hypertension. Cardiology 1995;86(suppl 1):9-15.

40. Galiè N, Hinderliter AL, Torbicki A, Fourme T, Simonneau G, Pulido T, Espinola-Zavaleta N, Rocchi G, Manes A, Frantz R, Kurzyna M, Nagueh SF, Barst R, Channick R, Dujardin K, Kronenberg A, Leconte I, Rainisio M, Rubin L. Effects of the oral endothelin-receptor antagonist Bosentan on echocardiographic and Doppler measures in patients with pulmonary arterial hypertension. J Am Coll Cardiol 2003;41:1380-6.

41. Dingemanse J, van Giersbergen LM. Clinical pharmacology of bosentan, a dual endothelin receptor antagonist. Clin Pharmacochinet 2004;43(15):1089-1115.

42. Galiè N, Ghofrani HA, Torbicki A, Barst RJ, Rubin LJ, Badesch D, Fleming T, Parpia T, Burgess G, Branzi A, Grimminger F, Kurzyna M, Simonneau G, for the Sildenafil Use in Pulmonary Arterial Hypertension (SUPER) Study Group. Sildenafil citrate therapy for pulmonary arterial hypertension. N Engl J Med 2005;353:2148-57.

43. Wilkins MR, Paul GA, Strange JW, Tunariu N, Gin-Sing W, Banya WA, Westwood MA, Stefanidis A, Ng LL, Pennell DJ, Mohiaddin RH, Nihoyannopoulos P, Gibbs JSR. Sildenafil versus endothelin receptor antagonist for pulmonary hypertension (SERAPH) study. Am J Respir Crit Care Med 2005;171:1292-7.

44. Kasimir MT, Seebacher G, Jaksch P, Winkler G, Schmid K, Marta GM, Simon P, Klepetko W. Reverse cardiac remodelling in patients with primary pulmonary hypertension after isolated lung transplantation. Eur J Cardiothorac Surg 2004;26:776-81.

45. Nagaya N, Kangawa K, mKanda M, Uematsu M, Horio T, Fukuyama N, Hino J, Harada-Shiba M, Okumura H, Tabata Y, Mochizuki N, Chiba Y, Nishioka K, Miyatake K, Asahara T, Hara H, Mori H. Hybrid cell-gene therapy for pulmonary hypertension based on phagocytosing action of endothelial progenitor cells. Circulation 2003;108:889-95.

46. Raoul W, Wagner-Ballon O, Saber G, Hulin A, Marcos E, Giraudier S, Vainchenker W, Adnot S, Eddahibi S, Maitre B. Effects of bone marrow-derived cells on monocrotaline- and hypoxia-induced pulmonary hypertension in mice. Resp Res 2007;8:8.

47. Campbell AIM, Kuliszewski MA, Stewart DJ. Cell-based gene transfer to the pulmonary vasculature. Endothelial nitric oxide synthase overexpression inhibits monocrotaline-induced pulmonary hypertension. Am J Respir Cell Mol Biol 1999; 21: 567–75.

48. Zhao YD, Courtman DW, Ng DS, Robb MJ, Deng YP, Trogadis J, Han RN, Stewart DJ. Microvascular regeneration in established pulmonary hypertension by angiogenic gene transfer. Am J Respir Cell Mol Biol 2006;35:182-9.

49. Baber SR, Deng, Master RG, Bunnell BA, Taylor BK, Murthy SN, Hyman AL, Kadowitz PJ. Intratracheal mesenchymal stem cell administration attenuates monocrotaline induced pulmonary hypertension and endothelial dysfunction. Am J Physiol Heart Circ Physiol 2007; 292: H1120–H1128.

50. Patel KM, Crisostomo P, Lahm T, Markel T, Herring C, Wang M, Meldrum KK, Lillemoe KD, Meldrum DR. Mesenchymal stem cells attenuate hypoxic pulmonary vasoconstriction by a paracrine mechanism. J Surg Res 2007;143:281-5.

51. Leung DW, Cachianes G, Kuang WJ, Goeddel DV, Ferrara N. Vascular endothelial growth factor is a secreted angiogenic mitogen. Science 1989; 246: 1306-9.

52. Flamme I, Breier G, Risau W. Vascular endothelial growth factor (VEGF) and VEGF receptor 2 (flk-1) are expressed during vasculogenesis and vascular differentiation in the quail embryo. Dev Biol 1995; 169: 699-712.

53. Asahara T, Murohara T, Sullivan A, Silver M, van der Zee R, Li T, Witzenbichler B, Schatteman G, Isner JM. Isolation of putative progenitor endothelial cells for angiogenesis. Science 1997; 275: 964-7.

54. Takahashi T, Kalka C, Masuda H, Chen D, Silver M, Kearney M, Magner M, Isner JM, Asahara T. Ischemia- and cytokine-induced mobilization of bone marrow-derived endothelial progenitor cells for neovascularization. Nat Med 1999; 5: 434-8.

55. Campbell AIM, Zhao Y, Sandhu R, Stewart DJ. Cell-based gene transfer of vascular endothelial growth factor attenuates monocrotaline-induced pulmonary hypertension. Circulation 2001; 104: 2242-8.

56. Fujita M, Mason RJ, Cool C, Shannon JM, Hara N, Fagan KA. Pulmonary hypertension in TNFα-overexpressing mice is associated with decreased VEGF gene expression. J Appl Physiol 2002;93:2162-70.